Curr Radiol Rep (2017) 5:55
DOI 10.1007/s40134-017-0252-6

New Imaging Techniques for Atherosclerotic Plaque Characterization

Francesco Lavra[1,2] · Carlo N. De Cecco[1] · Akos Varga-Szemes[1] · Domenico De Santis[1,3] · Moritz H. Albrecht[1,4] · Virginia W. Lesslie[1] · Marly van Assen[1,5] · Philipp von Knebel Doeberitz[1] · Domenico Mastrodicasa[1,6] · Marwen Eid[1] · Georg Apfaltrer[1,7] · Seth Stalcup[8] · Richard R. Bayer[1,9] · Luca Saba[2] · U. Joseph Schoepf[1]

Published online: 4 September 2017

Abstract
Purpose Previously, the imaging of atherosclerotic plaque has been limited to the assessment of vessel stenosis and occlusion. However, recent technological advances have allowed for more detailed plaque characterization. This article will address recent advancements in plaque characterization using both invasive and noninvasive techniques, as well as potential improvements in patient evaluation and targeted therapies.
Recent Findings Recent findings have demonstrated that plaque composition affects plaque vulnerability, or the propensity of a plaque to rupture and cause acute thrombus formation with potentially life-threatening downstream implications.
Summary Newly introduced invasive and noninvasive techniques allow for a comprehensive assessment of atherosclerotic plaque to classify high-risk patients requiring more intensive therapy.

Keywords Vulnerable plaque · Plaque characterization · Atherosclerosis · Computed tomography · Intravascular ultrasound · Magnetic resonance imaging

Introduction

Atherosclerosis is a systemic inflammatory disease and is the leading cause of morbidity and mortality in Western society [1, 2]. Plaque formation evolves gradually through different stages of development, including endothelial dysfunction, cholesterol deposition, inflammation, immune response, extracellular matrix formation, neoangiogenesis, and thrombosis [3]. Plaque rupture and underlying endothelial erosion are the most frequent causes of luminal thrombosis, often leading to acute ischemic events [3].

This article is part of the Topical Collection on *New Imaging Technologies*.

✉ U. Joseph Schoepf
schoepf@musc.edu

[1] Division of Cardiovascular Imaging, Department of Radiology and Radiological Science, Medical University of South Carolina, Charleston, SC, USA

[2] Department of Radiology, Azienda Ospedaliero Universitaria (A.O.U.), Cagliari, Italy

[3] Department of Radiological Sciences, Oncological and Pathological Sciences, University of Rome Sapienza, Latina, Italy

[4] Department of Diagnostic and Interventional Radiology, University Hospital Frankfurt, Frankfurt, Germany

[5] Center for Medical Imaging, University Medical Center Groningen, North East Netherlands, Groningen, The Netherlands

[6] Section of Diagnostic Imaging and Therapy – Radiology Division, Department of Neuroscience, Imaging and Clinical Science, "G. d'Annunzio" University, Chieti, Italy

[7] Division of Pediatric Radiology, Department of Radiology, Medical University of Graz, Graz, Austria

[8] Department of Radiology, Medical University of South Carolina, Charleston, SC, USA

[9] Division of Cardiology, Medical University of South Carolina, Charleston, SC, USA

The simple anatomical evaluation of stenosis has not proven effective in characterizing certain plaque features linked to the risk of rupture [4–8] or in the quantification of disease activity, another important factor in overall risk assessment [9]. For these reasons, atherosclerotic plaque assessment has recently evolved from mere anatomical imaging to a more comprehensive assessment of plaque composition to detect plaque vulnerability and disease activity.

The purpose of this review is to summarize recent developments in atherosclerosis imaging, including techniques to examine the pathophysiological processes involved in plaque maturation and rupture, and to offer insight into future directions for the treatment and diagnosis of atherosclerotic disease.

Plaque Vulnerability

Plaque vulnerability is linked to a loss of plaque structural stability, which may be caused by reduced collagen content in a thin fibrous cap surrounding a highly thrombogenic core [1]. Structural instability may also be caused by metabolic or immune insults that compromise the endothelial surface overlying a plaque, making it particularly susceptible to disease progression or rupture [1].

Among vulnerable plaques, a specific subtype that is responsible for the majority of plaque ruptures deserves special mention: Thin-cap fibroatheroma (TCFA) is characterized by a thin fibrous cap (<65 μm), a large lipid-rich necrotic core [(LRC) total plaque volume >40%], macrophage infiltration and inflammation, vascular remodeling, densely calcified areas (>10%), and a heavy plaque burden [10].

Invasive Diagnostic Techniques

Invasive coronary angiography (ICA) remains the gold standard for the evaluation of the presence, distribution, and severity of atherosclerotic lesions. However, ICA does not allow for the identification of nonstenotic vulnerable plaques that remain clinically silent before eventually causing an acute event [10].

Virtual histology-intravascular ultrasound (VH-IVUS), near-infrared spectroscopy (NIRS), and optical coherence tomography (OCT) are techniques performed during ICA that can characterize plaque and detect specific features that increase the risk of rupture.

Intravascular Ultrasound

While grayscale IVUS uses the amplitude of reflected ultrasound waves to generate an image [11] (Fig. 1), VH-IVUS utilizes iterative-based automated processing of the reflected ultrasound backscatter signal. This technical feature allows for an improved delineation of different plaque components, including fibrous tissue, fibro-fatty tissue, an LRC, and dense calcifications [12]. An automated pullback device withdraws the VH-IVUS catheter (either a 20-MHz phased array or a 45-MHz rotational array) at a preset speed (e.g., 0.5 mm s^{-1}) to enable the acquisition of a cylindrical dataset across the artery length and including the site of the lesion.

Depending on tissue type, concordance between VH-IVUS and in vitro histopathology following atherectomy ranges from 87.1 to 96.5% [10, 13–15]. However, one study demonstrated discrepant results between IVUS and in vitro histology for the identification of LRC [16].

Due to the limited spatial resolution of IVUS (100–200 μm), TCFA is more difficult to define. Thus, most studies adopt a simplified definition that characterizes any focal, LRC lesion without evidence of overlying fibrous tissue as TCFA [10, 17]. An in vivo study showed a correlation between TCFA detected with IVUS and major adverse cardiac events (MACE), defined as mortality, acute coronary syndrome (ACS), or unplanned revascularization [18]. Specifically, the study enrolled patients who underwent ICA for ACS or stable angina. The presence of TCFA was determined using VH-IVUS in nonculprit coronary arteries. Results suggest that the presence of TCFA is strongly and independently associated with the occurrence of MACE within 1 year of the procedure (adjusted hazard ratio [HR] 1.98), proving particularly true for TCFA with a large plaque burden (adjusted HR 2.90).

For the evaluation of drug-eluting stents, a recent study has shown the utility of IVUS during percutaneous coronary interventions (PCI). Results demonstrated a reduction in MACE following IVUS-guided PCI versus angiographically guided PCI (odds ratio [OR] 0.79) [19]. In addition, VH-IVUS may be useful to evaluate changes in plaque composition following statin therapy, with one study showing a reduction of LRC volume, total plaque burden, and TCFA at 1-year follow-up in nonculprit lesions [20].

Despite the usefulness of VH-IVUS in the evaluation of the coronary artery lumen, wall, and associated plaques for pre- and postintervention assessment of lesion morphology, this technique is hampered by major drawbacks. Specific shortcomings include limited spatial resolution, restricted ability to visualize the thin fibrous cap, and poor sensitivity in the depiction of lipid-rich plaque (LRP) [10, 17].

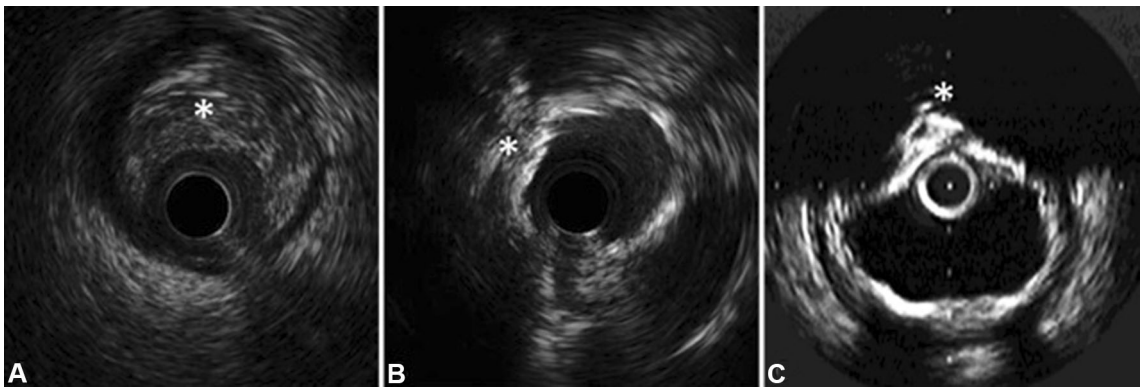

Fig. 1 Example of various atherosclerotic plaques classified by intravascular ultrasound (IVUS) showing **a** a fibro-fatty plaque. **b** a fibro-calcific plaque. **c** a calcified plaque. The different types of plaque are indicated by an *asterisk* in each of the figures

Near-Infrared Spectroscopy

NIRS is a well-established technique that is used to determine the chemical composition of a particular sample. Due to this capability, NIRS proves useful in the characterization of atherosclerotic plaque, specifically aiding in the detection of LRP in the coronary vasculature [21]. In recently developed catheter-based NIRS systems, optical fibers emit and receive near-infrared light (λ_o = 0.8–2.5 - μm). Each component of the atherosclerotic plaque absorbs the emitted wavelengths in a specific pattern unique to its composition, and the reflected signals from the tissue are then converted to spectra [21, 22]. The physical acquisition of these spectra with an automated pullback device, in tandem with their processing by a transformation algorithm, allows one to determine the likelihood that LRP is present in the vessel wall. These probabilities are depicted as a chemogram, with red pixels indicating low probability and yellow pixels indicating high probability [10].

In clinical studies utilizing NIRS, lipid burden is estimated in a semiquantitative manner through the maximum lipid core burden index (LCBI), which is calculated as a ratio between the number of yellow pixels and the total number of valid pixels (red and yellow) in any 4-mm section of the artery (maxLCBI4mm) [23, 24•, 25•, 26, 27]. New NIRS catheters employ IVUS technology to provide the operator with information regarding the composition as well as the structure of plaques within the coronary arteries [28].

In three studies, Madder et al. demonstrated [24•, 25•, 29] that NIRS imaging can identify vulnerable plaques with an increased risk of triggering a future myocardial infarction (MI) at culprit lesions. In a cohort of 20 patients diagnosed with acute ST-elevation myocardial infarction (STEMI), investigators showed that a maxLCBI4 mm threshold >400 distinguished STEMI culprit segments from regions free of large LRP, with a sensitivity of 85% and specificity of 98%, as determined by histology [24•].

In 81 patients diagnosed with either non-STEMI (NSTEMI) or unstable angina who underwent culprit vessel NIRS imaging prior to stenting, a maxLCBI4mm threshold ≥400 provided a sensitivity of 63.6% and specificity of 94.0% in differentiating culprit from non-culprit segments in the NSTEMI cohort. For the detection of culprit segments in patients with unstable angina, a sensitivity of 38.5% and specificity of 89.8% was achieved using the same threshold [25•].

In a selected cohort of five patients resuscitated from cardiac arrest, a maxLCBI4mm threshold ≥400 was detected by NIRS at each culprit segment [29]. Stone et al. showed that a maxLCBI4mm threshold ≥600 was associated with peri-procedural myocardial necrosis in 24.7% of cases prior to stent implantation of a single native coronary lesion [26].

The main limitation of NIRS is that it only provides compositional information (i.e., the probability of the presence of a LRP at a given site), without any quantitative or morphological data (e.g., lumen size, plaque burden) [27].

Optical Coherence Tomography

OCT uses a low-coherence, near-infrared light source (center wavelength, λ_o = 1.3 μm), which is directed toward and reflected from the vessel wall to generate an image [30]. Its exceptional spatial resolution (<10 μm axially; 20–40 μm laterally) allows for precise identification of vulnerable atherosclerotic plaque features associated with a high risk of rupture, including fibrous, lipid-rich, or calcified lesions, red and white thrombus, and macrophage infiltration [31].

Compared with histopathology, OCT achieved optimal results in the evaluation of plaque composition, with a pooled sensitivity and specificity in ranges of 87–92 and 94–100%, respectively [32].

OCT can be helpful for the in vivo identification of the thin fibrous cap of TCFA, and calcified and eroded plaques, all of which are considered high-risk features [31]. More specifically, plaque erosion has been detected by OCT in 20–30% of culprit lesions, while OCT-determined calcified nodules, indicating fibrous cap disruption over sites of calcified plaque, had an incidence of 7.9% in patients with ACS [33].

Another study demonstrated that fibrous cap thickness, as determined by OCT, is the best predictor of peri-procedural MI during PCI in patients with coronary artery disease (CAD). This was compared to both IVUS-measured plaque burden and NIRS-measured LCBI (OR 0.90), as well as cardiac troponin elevations greater than 5 times the upper limit (OR 0.91) [34•].

In order to prevent unnecessary stenting procedures, the use of OCT for the detection of plaque erosion may be particularly beneficial in STEMI patients without apparent disruption of the fibrous cap. A study performed in patients with ACS caused by subocclusive plaque demonstrated that patients with OCT-detected plaque erosion with an intact fibrous cap benefitted from dual antiplatelet therapy while avoiding PCI [35]. Moreover, OCT is useful in evaluating the efficacy of pharmacotherapeutic agents in stabilizing vulnerable plaques and preventing future rupture [36].

Limitations of OCT include a low penetration depth (1–2.5 mm), particularly through lipid-rich lesions, which hinders its capacity to determine plaque burden. In addition, OCT suffers from the presence of common imaging artifacts as well as the requirement for a blood-free field [30, 37, 38].

Non-invasive Diagnostic Techniques

The noninvasive imaging modalities currently available for atherosclerosis characterization include Computed Tomography (CT), Magnetic Resonance imaging (MRI), and Positron Emission Tomography (PET) (Figs. 2, 3). These various modalities can be used for the evaluation of multiple vascular regions, providing unique and complementary information regarding the biologic and morphologic features of plaque development [39].

Computed Tomography

Cardiac CT angiography (cCTA) has the ability to characterize atherosclerotic plaque based on the measurement of its density in Hounsfield Units (HU). The HU values traditionally used to classify plaque composition can be referenced in Table 1 [40, 41••].

Several studies have shown that traditional single energy (SE) cCTA has a high accuracy in the detection of major plaque features that are indicative of vulnerability and associated with the occurrence of acute events. Specific features of vulnerable plaques able to be detected on cCTA include low density values (Fig. 3), positive remodeling [(PR) defined as the ratio between vessel area at the plaque site and vessel area at a normal reference site >1], spotty calcifications [(SP) calcium deposits with an arc <90°], and the presence of a napkin-ring sign (a ring of attenuation values that are greater than those of the adjacent plaque tissues but <130 HU) (Fig. 4) [42–45].

A recent study analyzed the diagnostic performance of cCTA for the detection of obstructive CAD in 185 patients diagnosed with previous MI. Compared with ICA, cCTA showed a per-patient accuracy, sensitivity, specificity, negative predictive value (NPV), and positive predictive value (PPV) of 96.2, 100, 93.6, 100, and 91%, respectively. Moreover, cCTA performed well in predicting appropriate treatment strategies, achieving accuracy, sensitivity, specificity, NPV, and PPV of 95.1, 100, 90.1, 100, and 91.1%, respectively [43].

Nakazato et al. evaluated the performance of cCTA in the evaluation of plaque volume and composition using IVUS as the reference standard. Results from the study show a similar frequency of LRP (10% vs. 17%), PR (7% vs. 10%), and SP (27% vs. 33%) between cCTA and IVUS, respectively (all $p > 0.05$). Furthermore, an excellent correlation ($r = 0.95$) was found for calculations of plaque volume between independent observers and IVUS [44].

Moreover, in a cohort of 45 patients with ACS, cCTA demonstrated that culprit lesions were characterized by larger plaque volumes, higher remodeling indices, and a significantly higher presence of LRP with a density <30 or <60 HU, compared with nonculprit lesions [42]. A prospective study including 895 patients with suspected CAD undergoing cCTA showed that PR, LRP, and the napkin-ring sign were predictive factors for future ACS events. The presence of the napkin-ring sign proved to be an independent marker for future ACS events and significant prognostic implications, even in the absence of other high-risk features captured by cCTA [45].

These findings are validated by a retrospective study that assessed the discriminatory value of quantitative atherosclerotic plaque markers derived from a semiautomated cCTA approach in patients with first ACS compared to patients with stable CAD (Fig. 5) [41••]. Significantly higher median segment stenosis score, segment involvement score, noncalcified plaque volume, a higher prevalence of positive remodeling, and a longer median lesion length were observed in the ACS group (all $p < 0.05$). On a per-lesion basis, plaque quantification and characterization also showed significantly greater median total plaque volume, noncalcified plaque volume, plaque burden, vessel remodeling, atheromatous plaque length, and prevalence of

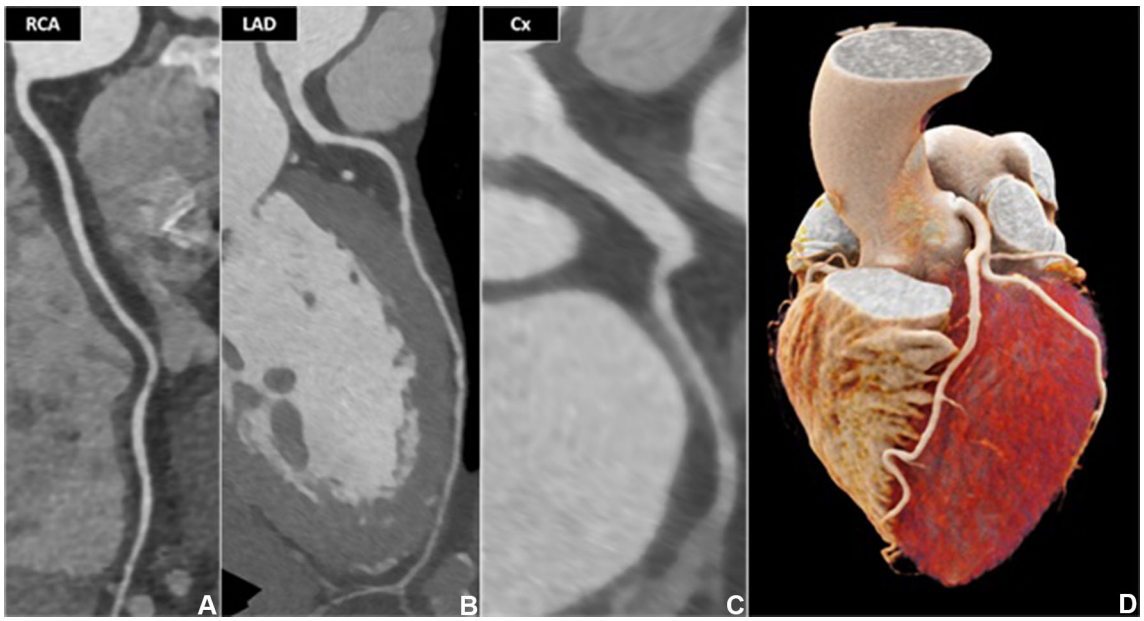

Fig. 2 cCTA of a 77-year-old man with acute chest pain. **a**–**c** Examples of curved multiplanar reformations showing no evidence of coronary stenosis (*RCA* right coronary artery, *LAD* left descending coronary artery, *Cx* left circumflex artery). **d** Cinematic rendering reformation showing no pathologic findings

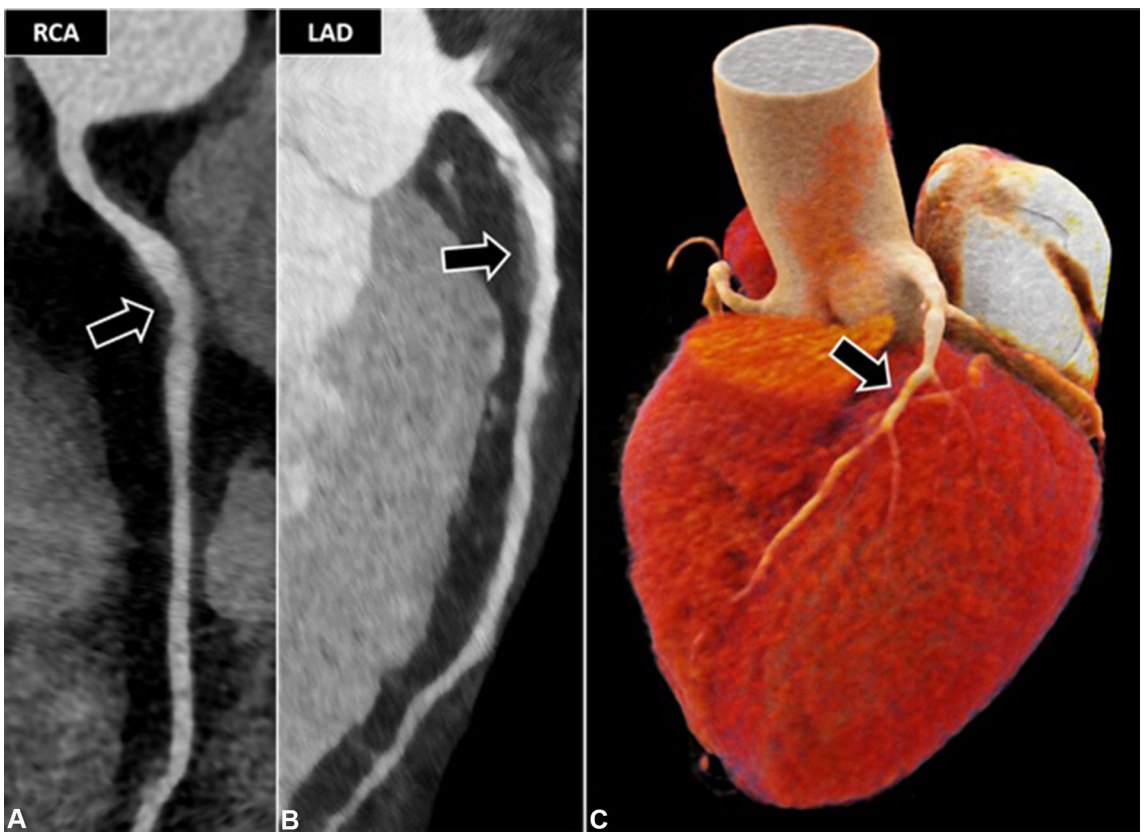

Fig. 3 cCTA of a 62-year-old man presenting with exertional chest pain with radiation to neck/jaw and left arm. **a**, **b** Curved multiplanar reformations depicting a nonsignificant stenosis of the right coronary artery (RCA, *arrow* in **a**), and a moderate stenosis in the proximal left anterior descending artery (LAD) caused by a lipid-rich plaque (*arrow* in **b**). **c** Cinematic rendering reformation demonstrating the resultant luminal narrowing of the LAD (*arrow*)

Table 1 Cutoff attenuation values for atherosclerotic plaque components and vessel lumen

Vessel components	Density values (HU)
Lipid-rich plaque	17–70
Fibrotic plaque	71–124
Intraluminal contrast material	125–511
Calcified plaque	>511

a napkin-ring sign in culprit versus nonculprit control lesions (all $p < 0.05$) [41••]. Furthermore, the inclusion of plaque markers to the Framingham risk score yielded the highest discriminatory value, emphasizing the clinical impact of plaque characterization as a tool for risk stratification [41••]. In agreement with these findings, a previous study has shown that machine learning algorithms that incorporate cCTA data as well as clinical parameters can increase the predictive value for all-cause mortality and patient outcomes [46]. Thus, this approach holds promise for the enhancement of plaque quantification techniques for risk stratification and decision-making in clinical practice.

Although an extensive body of evidence highlights the value of SEcCTA in the differentiation of plaque components, a previous meta-analysis showed a substantial overlap in attenuation values between LRP and fibrous plaque (47 ± 29 and 86 ± 29 HU, respectively). Findings also suggested that the optimal cutoff value for plaque differentiation is dependent on the CT system, acquisition parameters, and the specific vessel of interest [40, 47]. Due to this high degree of variability, future investigations are warranted to further define and generalize parameters for the discrimination of plaque components.

Despite these observations, it has been hypothesized that the tissue decomposition capabilities of dual energy CT (DECT) can overcome the system dependence of plaque characterization experienced in SECT. DECT material decomposition is based on the photoelectric effect, a photon absorption phenomenon dependent on the binding energy of the innermost electron shell (the k shell) for a particular material [48]. The maximum X-ray attenuation is observed at energy levels just above the binding energy (k edge) of different materials. Therefore, the simultaneous CT acquisition of two X-ray spectra at different peak tube voltages allows for the detection of specific attenuation characteristics based on differing energy levels for compounds such as calcium, iodine, uric acid, and iron [48].

However, a prospective study analyzing 20 patients showed that DECT and SECT had similar sensitivities (45 and 39%, respectively) for LRC detection, compared with IVUS as the reference standard [49]. Despite the use of postmortem samples, which effectively control for confounding variables linked to body habitus or motion, DECT mismatched 21% of noncalcified plaques [50]. These discrepant findings may be due to a lack of standardization in scanning protocol, as the systematic studies that evaluate the exact energy and/or material basis pairs that optimize plaque visualization have not yet been performed [51].

Plaque characterization with DECT has been evaluated in the carotid artery by Mannelli et al. who examined five ex vivo carotid endarterectomy samples using virtual monochromatic images (VMI). Images were reconstructed at energies between 40 and 140 keV, and conventional polychromatic spectrum CT was employed with peak beam energies of 80, 100, 120, and 140 kVp. Results were compared with histology. The VMI dataset achieved the highest sensitivity for the detection of calcifications (97.4% at 40 keV) and the most accurate size estimation obtained when using tube voltages between 80 and 100 keV [52]. Notably, DECT image acquisition allows for the retrospective generation of VMI at varying keV levels without

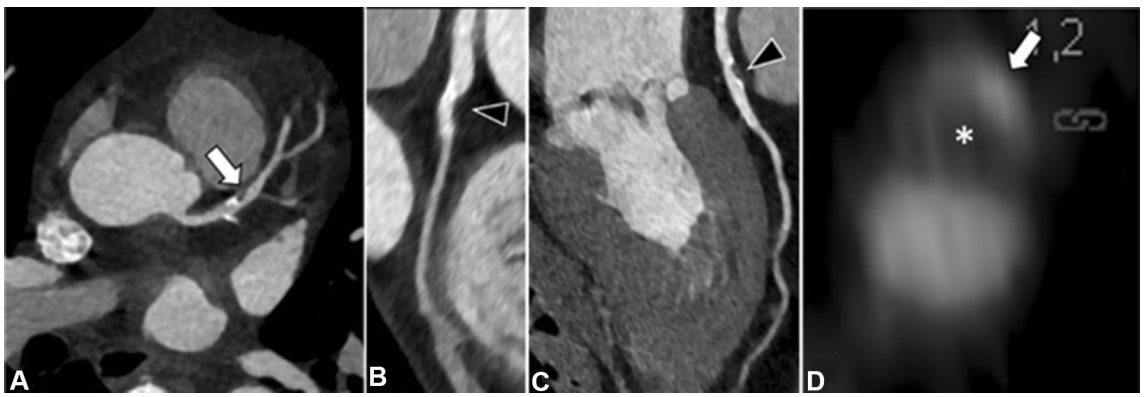

Fig. 4 cCTA images of a 56-year-old man with chest discomfort showing a coronary lesion with napkin-ring sign and positive remodeling. **a–c** Curved multiplanar reformation depicts the partially calcified plaque (*arrow* in **a**, *arrow head* in **b**, **c**) and the resultant partial lumen obstruction. **d** Axial reconstruction shows the circumferential hyper-dense outer rim of the plaque (*arrow*) encompassing the central hypo-dense necrotic core (*asterisk*). Notably, the total plaque area is greater than the residual lumen (positive remodeling)

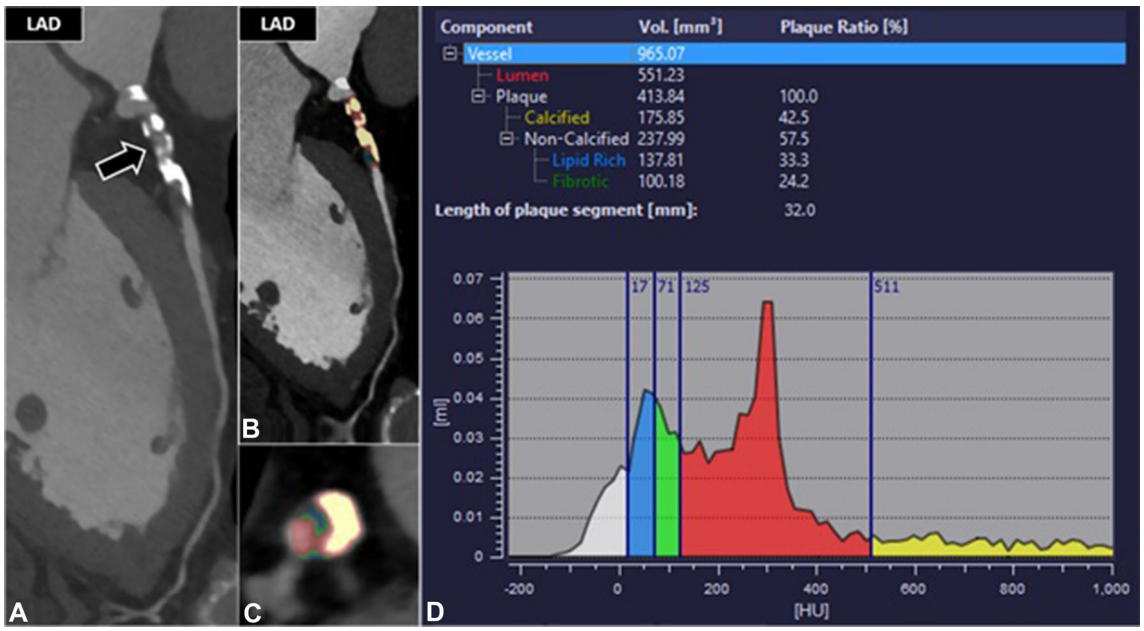

Fig. 5 cCTA study of a 73-year-old man presenting with NSTEMI. **a** cCTA displayed as an automatically generated curved multiplanar reformation demonstrates severe stenosis of the proximal tract of the left anterior descending artery (LAD, *arrow*). **b–d** Color-coded semiautomated plaque quantification of the target lesion depicting a mixed plaque

additional acquisitions, dose penalty, or contrast media requirements.

Magnetic Resonance Imaging

MRI is a noninvasive technique characterized by high soft-tissue contrast, in-plane resolution, and reproducibility. It functions by detecting the radiofrequency from protons following the application of a strong magnetic field and subsequently exploits the native relaxation properties of plaque components to differentiate among the various phenotypes. The use of nontargeted and targeted contrast materials modifies these native relaxation properties to help further delineate the various hallmarks of plaque vulnerability [53, 54] (Fig. 6).

Post-endarterectomy histopathologic analysis has identified intraplaque hemorrhage (IPH), ulceration, a thin fibrous cap, and an LRC as crucial plaque features observed on MRI that increase the risk of atherosclerotic plaque rupture [54, 55]. Table 2 lists conventional MRI plaque analysis findings and their corresponding sensitivity and specificity in the detection of major vulnerable plaque features [54–59].

Administration of gadolinium-based contrast media is essential for the differentiation of various plaque components, as it is effective in assessing plaque neovascularity and distinguishing between LRC and fibrous tissue on T1-weighted images. Indeed, LRC and IPH are avascular and do not show contrast enhancement, therefore allowing them to be differentiated from the enhanced fibrous cap of the plaque [60]. Furthermore, studies have demonstrated that plaque enhancement is associated with plaque vulnerability, neovascularization, macrophage infiltration, and symptomatic events [55]. Specifically, neovascularity and macrophage infiltration are observed in 97 and 87% of regions characterized by contrast enhancement, respectively [61].

Studies with high reproducibility and reliability have shown that the adventitial volume transfer coefficient (K_{trans}), calculated using dynamic contrast-enhanced (DCE) MRI, is strongly associated with neovascularity and inflammation [60, 62, 63]. Furthermore, plaque enhancement on DCE MRI is significantly associated with ipsilateral ischemic events, independent of stenosis severity [61, 62].

Certain MRI-detectable plaque features have been shown to be negative prognostic factors for plaque rupture. A systematic review of nine studies involving 779 subjects demonstrated that LRC, IPH, and thinning or rupture of the fibrous cap had hazard ratios (HR) of 3.00, 4.59, and 5.93, respectively, for transient ischemic attack (TIA) or stroke [64••]. A recent meta-analysis included 689 subjects presenting with TIA or asymptomatic moderate carotid stenosis, as determined by sonography, who underwent carotid MRI. At mean follow-up of 19.6 months, a total of 108 cerebrovascular events occurred (15.7%), and the presence of IPH was associated with approximately six times the risk for future adverse events (HR 5.69). In

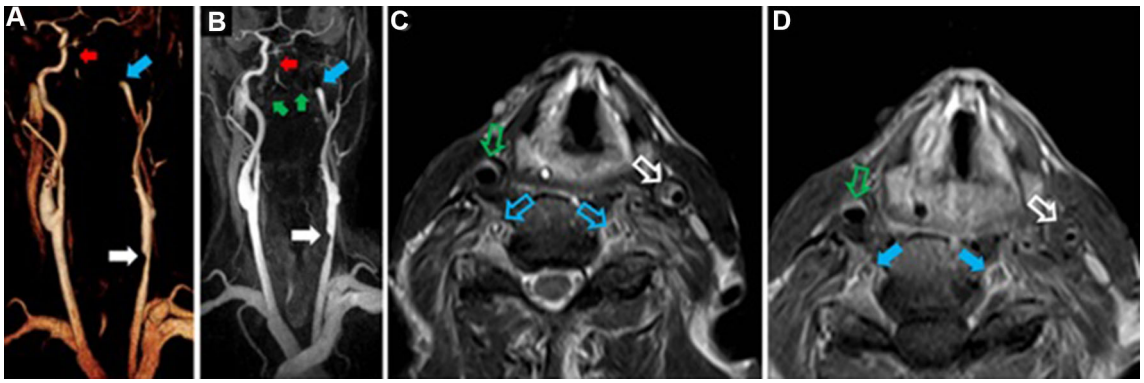

Fig. 6 MRI and MRA visualization of atherosclerotic disease in a 74-year-old man. 3D reformations (**a**) and maximum intensity projection (**b**) images showing severe stenosis of the left common carotid artery (*white arrows*); total occlusion of the left internal carotid artery (*blue arrows*); bilateral occlusion of the vertebral arteries (*green arrows*); and occlusion of the basilar artery (*red arrows*). Axial T2-weighted (**c**) and postcontrast T1-weighted (**d**) images showing a heterogeneous atheromatous plaque in the left common carotid artery (*white open arrows*). The lack of flow voids in the vertebral arteries (*blue open arrows*) indicates slow arterial blood flow. Atherosclerotic plaque can also be visualized in the right common carotid artery with normal flow void (*green open arrows*)

Table 2 Conventional MRI findings for atherosclerotic plaque components

Vulnerable plaque feature	MRI sequences	MRI finding	Sensitivity (%)	Specificity (%)
Plaque ulceration	3D TOF, T1w, T2w, PD, black blood MRA, CET1w	Plaque surface disruption	80	70
LRC	T1w	Hyperintense	82–100	40–10
Calcification	All contrast images	Hypointense	76–84	86–94
IPH	T1w, Tw fat suppression, TOF MRA	IPH <6 weeks- hyperintense	82–97	74–100
		IPH >6 weeks- hypointense		

TOF time of flight, *PD* proton density, *MRA* magnetic resonance angiography, *CET1w* contrast enhancement T1 weighted, *LRC* lipid-rich necrotic core, *IPH* intraplaque hemorrhage

addition, IPH was associated with a 17.7% risk of stroke per year of follow-up [65].

MRI has also been utilized to assess the effects of pharmacological therapy on plaque stability [66]. A recent study investigated a cohort of 25 patients with symptomatic low-grade carotid stenosis (50%) as well as both high-signal plaque and expansive remodeling observed on MRI. On T1-weighted images, the presence of IPH was associated with a high rate of ischemic events, regardless of whether antithrombotic or statin therapy was used. These patients underwent carotid endarterectomy with a subsequent reduction in the rate of future ischemic events [67].

A retrospective study analyzed 205 patients with high-grade carotid artery stenosis scheduled for elective revascularization with stenting or endarterectomy. Patients were divided into two groups: one group was treated with standard of care, while the other underwent time of flight MR angiography as a gatekeeper for subsequent endarterectomy. Decisions for further treatment in the MRI cohort were based on the presence of a high-intensity signal in the plaque, as this is considered a sign of instability. Patients without MRI had a significantly higher incidence (9.5% vs. 1.8%, $p = 0.034$) of peri-procedural adverse events compared with patients in which MRI determined whether endarterectomy was performed. In addition, MRI-based treatment selection was the only independent predictor of peri-procedural events ($p = 0.043$) in this study [68••].

Compared with the carotid arteries, the study of coronary vessel walls with cardiac Magnetic Resonance imaging (cMRI) is technically more demanding due to the high spatial resolution required to properly study the small luminal area and thin wall [69].

Since cMRI image resolution is proportional to scan time, an extended scan may be necessary to reach adequate spatial resolution, thus resulting in a higher susceptibility to motion-related artifacts such as ghosting and blurring [69].

This technical challenge constitutes an unsolved limitation of coronary artery plaque characterization with MRI.

Positron Emission Tomography-Computed Tomography

PET allows for the detection of underlying pathophysiological processes associated with atherogenesis and subsequent plaque destabilization, particularly through the use of radiotracers specific to metabolic processes characteristic of plaque development [70].

F-flurodeoxyglucose (FDG) is utilized to detect vascular inflammation in the context of FDG-PET/CT [71]. Moreover, an investigation performed by Figueroa et al. including 513 patients with recent stroke demonstrated that active carotid inflammation in the context of atherosclerotic disease acts as an independent predictor of recurrent stroke [72].

Atheroma inflammation may favor plaque microcalcification deposits, which can predispose plaques to rupture due to mechanical disruption of the fibrous cap or interaction of preexisting inflammation with the calcium deposit. This process can be detected using 18F-sodium fluoride (NaF), since this radiotracer replaces the hydroxyl group of hydroxylapatite at sites of mineralization, allowing for accurate evaluation [71].

A recent study corroborated the clinical use of NaF-PET imaging, demonstrating in histological specimens that NaF was preferentially colocalized to areas of pathological mineralization, indicative of emerging calcification and active unstable atherosclerosis. The grade of NaF adsorption is proportional to the surface area of the mineralized spots. Consequently, the convex surface structure of microcalcifications allows for the increased fluoride bonding relative to macrocalcifications which are characterized by a flatter appearance and reduced surface area [73•].

In addition, other experiments showed a lack of colocalization between regions of macrocalcification and fluoride uptake. Notably, the tracer showed an inverse relationship to plaque calcium score. This finding suggests that microcalcification represents an active mineralization process rather than the macrocalcification burden [74–76]. Furthermore, NaF-PET/CT has proven to be a precise imaging technique, reaching an intraclass correlation coefficient of 0.99 [77].

In addition, PET/CT can be applied to measure the effects of pharmacological treatments on plaque characteristics. Specifically, atheroma stabilization due to the anti-inflammatory effects of statin therapy can be observed as a reduction in FDG uptake in serial acquisitions. This may represent a potential benefit of statin therapy beyond its lipid reducing effect [78, 79].

Despite its notable role in plaque characterization, the implementation of PET imaging in atherosclerosis is limited by its relatively low availability, high cost, increased radiation exposure, and low spatial resolution ($\sim$3 mm). In addition, in FDG imaging, the proximity of a hand-drawn region of interest to tissues with high resting metabolic activity such as ganglia or myocardium may hinder inflammation detection [70].

Future Directions

Current research in plaque imaging is largely focused on developing noninvasive methods to guide treatment decisions for patients at risk of an acute event. In terms of coronary atherosclerosis, CT is the most promising technique to meet this demand. The interplay of semiautomated plaque characterization, artificial intelligence, and noninvasive quantification of fractional flow reserve has the potential to yield a comprehensive assessment of CAD that allows for the identification of functionally significant plaque.

Development of new PET tracers is a particularly promising avenue for clinical application, largely due to their capacity to highlight underlying pathologic processes linked to plaque vulnerability. Hybrid PET/MRI is an innovative technique in which the complimentary nature of MRI and PET may allow for the simultaneous assessment of plaque morphology and metabolism [80, 81].

Despite the potential advances of the aforementioned techniques, the translation of these into a comprehensive decision-making protocol that incorporates multiple imaging modalities must be continually re-evaluated with every new technological improvement.

Conclusion

New developments in imaging and the characterization of atherosclerotic plaque have improved our knowledge regarding the pathophysiology of plaque development and rupture, demonstrating that plaque assessment cannot be based solely on anatomical parameters. Promising clinical implications of these improvements have the potential to benefit a large patient population, with added benefits to overall patient cost. Specifically, the combination of multiple noninvasive imaging techniques could be used to develop clinical strategies that help guide future treatment decisions, including progression to invasive imaging and intervention. Despite these potential benefits, further prospective clinical trials must be performed to demonstrate how incorporation of these new techniques into clinical practice affects patient outcomes.

Funding U. Joseph Schoepf is a consultant for and/or receives institutional research support from Astellas, Bayer, GE, Guerbet, and Siemens Healthineers, and is a section editor for *Current Radiology Reports*.

Compliance with Ethical Guidelines

Conflict of interest Francesco Lavra, Carlo N. De Cecco, Akos Varga-Szemes, Domenico De Santis, Moritz H. Albrecht, Virginia W. Lesslie, Marly van Assen, Philipp von Knebel Doeberitz, Domenico Mastrodicasa, Marwen Eid, Georg Apfaltrer, Seth Stalcup, Richard R. Bayer, and Luca Saba each declares no potential conflicts of interest.

Human and Animal Rights and Informed Consent This article does not contain any studies with human or animal subjects performed by any of the authors.

References

Papers of particular interest, published recently, have been highlighted as:
- • Of importance
- •• Of major importance

1. Hansson GK, Libby P, Tabas I. Inflammation and plaque vulnerability. J Intern Med. 2015;278(5):483–93. doi:10.1111/joim.12406.
2. Libby P, Tabas I, Fredman G, Fisher EA. Inflammation and its resolution as determinants of acute coronary syndromes. Circ Res. 2014;114(12):1867–79. doi:10.1161/CIRCRESAHA.114.302699.
3. Falk E, Nakano M, Bentzon JF, Finn AV, Virmani R. Update on acute coronary syndromes: the pathologists' view. Eur Heart J. 2013;34(10):719–28. doi:10.1093/eurheartj/ehs411.
4. Freilinger TM, Schindler A, Schmidt C, Grimm J, Cyran C, Schwarz F, et al. Prevalence of nonstenosing, complicated atherosclerotic plaques in cryptogenic stroke. JACC Cardiovasc Imaging. 2012;5(4):397–405. doi:10.1016/j.jcmg.2012.01.012.
5. Gupta A, Gialdini G, Lerario MP, Baradaran H, Giambrone A, Navi BB, et al. Magnetic resonance angiography detection of abnormal carotid artery plaque in patients with cryptogenic stroke. J Am Heart Assoc. 2015;4(6):e002012. doi:10.1161/JAHA.115.002012.
6. Ota H, Magalhaes MA, Torguson R, Negi S, Kollmer MR, Spad MA, et al. The influence of lipid-containing plaque composition assessed by near-infrared spectroscopy on coronary lesion remodelling. Eur Heart J Cardiovasc Imaging. 2016;17(7):821–31. doi:10.1093/ehjci/jev221.
7. Motoyama S, Ito H, Sarai M, Kondo T, Kawai H, Nagahara Y, et al. Plaque characterization by coronary computed tomography angiography and the likelihood of acute coronary events in mid-term follow-up. J Am Coll Cardiol. 2015;66(4):337–46. doi:10.1016/j.jacc.2015.05.069.
8. Puchner SB, Liu T, Mayrhofer T, Truong QA, Lee H, Fleg JL, et al. High-risk plaque detected on coronary CT angiography predicts acute coronary syndromes independent of significant stenosis in acute chest pain: results from the ROMICAT-II trial. J Am Coll Cardiol. 2014;64(7):684–92. doi:10.1016/j.jacc.2014.05.039.
9. Dweck MR, Aikawa E, Newby DE, Tarkin JM, Rudd JH, Narula J, et al. Noninvasive molecular imaging of disease activity in atherosclerosis. Circ Res. 2016;119(2):330–40. doi:10.1161/CIRCRESAHA.116.307971.
10. Batty JA, Subba S, Luke P, Gigi LW, Sinclair H, Kunadian V. Intracoronary imaging in the detection of vulnerable plaques. Curr Cardiol Rep. 2016;18(3):28. doi:10.1007/s11886-016-0705-1.
11. Fujii K, Hao H, Ohyanagi M, Masuyama T. Intracoronary imaging for detecting vulnerable plaque. Circ J. 2013;77(3):588–95.
12. Nair A, Margolis MP, Kuban BD, Vince DG. Automated coronary plaque characterisation with intravascular ultrasound backscatter: ex vivo validation. EuroIntervention. 2007;3(1):113–20.
13. Nasu K, Tsuchikane E, Katoh O, Vince DG, Virmani R, Surmely JF, et al. Accuracy of in vivo coronary plaque morphology assessment: a validation study of in vivo virtual histology compared with in vitro histopathology. J Am Coll Cardiol. 2006;47(12):2405–12. doi:10.1016/j.jacc.2006.02.044.
14. Watson RJ, McLean CC, Moore MP, Spencer T, Salter DM, Anderson T, et al. Classification of arterial plaque by spectral analysis of in vitro radio frequency intravascular ultrasound data. Ultrasound Med Biol. 2000;26(1):73–80.
15. Nair A, Kuban BD, Tuzcu EM, Schoenhagen P, Nissen SE, Vince DG. Coronary plaque classification with intravascular ultrasound radiofrequency data analysis. Circulation. 2002;106(17):2200–6.
16. Brugaletta S, Cola C, Martin-Yuste V, Vilahur G, Oriol J, Padro T, et al. Qualitative and quantitative accuracy of ultrasound-based virtual histology for detection of necrotic core in human coronary arteries. Int J Cardiovasc Imaging. 2014;30(3):469–76. doi:10.1007/s10554-014-0372-5.
17. Rodriguez-Granillo GA, Garcia-Garcia HM, Mc Fadden EP, Valgimigli M, Aoki J, de Feyter P, et al. In vivo intravascular ultrasound-derived thin-cap fibroatheroma detection using ultrasound radiofrequency data analysis. J Am Coll Cardiol. 2005;46(11):2038–42. doi:10.1016/j.jacc.2005.07.064.
18. Cheng JM, Garcia-Garcia HM, de Boer SP, Kardys I, Heo JH, Akkerhuis KM, et al. In vivo detection of high-risk coronary plaques by radiofrequency intravascular ultrasound and cardiovascular outcome: results of the ATHEROREMO-IVUS study. Eur Heart J. 2014;35(10):639–47. doi:10.1093/eurheartj/eht484.
19. Jang JS, Song YJ, Kang W, Jin HY, Seo JS, Yang TH, et al. Intravascular ultrasound-guided implantation of drug-eluting stents to improve outcome: a meta-analysis. JACC Cardiovasc Interv. 2014;7(3):233–43. doi:10.1016/j.jcin.2013.09.013.
20. Park SJ, Kang SJ, Ahn JM, Chang M, Yun SC, Roh JH, et al. Effect of statin treatment on modifying plaque composition: a double-blind, randomized study. J Am Coll Cardiol. 2016;67(15):1772–83. doi:10.1016/j.jacc.2016.02.014.
21. Jaguszewski M, Klingenberg R, Landmesser U. Intracoronary near-infrared spectroscopy (NIRS) imaging for detection of lipid content of coronary plaques: current experience and future perspectives. Curr Cardiovasc Imaging Rep. 2013;6:426–30. doi:10.1007/s12410-013-9224-2.
22. Waxman S, Dixon SR, L'Allier P, Moses JW, Petersen JL, Cutlip D, et al. In vivo validation of a catheter-based near-infrared spectroscopy system for detection of lipid core coronary plaques: initial results of the SPECTACL study. JACC Cardiovasc Imaging. 2009;2(7):858–68. doi:10.1016/j.jcmg.2009.05.001.
23. Madder RD, Smith JL, Dixon SR, Goldstein JA. Composition of target lesions by near-infrared spectroscopy in patients with acute coronary syndrome versus stable angina. Circ Cardiovasc Interv. 2012;5(1):55–61. doi:10.1161/CIRCINTERVENTIONS.111.963934.
24. • Madder RD, Goldstein JA, Madden SP, Puri R, Wolski K, Hendricks M, et al. Detection by near-infrared spectroscopy of large lipid core plaques at culprit sites in patients with acute ST-

segment elevation myocardial infarction. JACC Cardiovasc Interv. 2013;6(8):838–46. doi:10.1016/j.jcin.2013.04.012. *This article is important because it demonstrates that NIRS may allow for the delineation of culprit vs. non-culprit atherosclerotic lesions in patients with stable/acute coronary artery disease, potentially allowing a site-specific method for predicting future acute coronary events.*

25. • Madder RD, Husaini M, Davis AT, VanOosterhout S, Harnek J, Gotberg M, et al. Detection by near-infrared spectroscopy of large lipid cores at culprit sites in patients with non-ST-segment elevation myocardial infarction and unstable angina. Catheter Cardiovasc Interv. 2015;86(6):1014–21. doi:10.1002/ccd.25754. *This article is important because it demonstrates that NIRS may allow for the delineation of culprit vs. non-culprit atherosclerotic lesions in patients with stable/acute coronary artery disease, potentially allowing a site-specific method for predicting future acute coronary events.*
26. Stone GW, Maehara A, Muller JE, Rizik DG, Shunk KA, Ben-Yehuda O, et al. Plaque characterization to inform the prediction and prevention of periprocedural myocardial infarction during percutaneous coronary intervention: the CANARY trial (coronary assessment by near-infrared of atherosclerotic rupture-prone yellow). JACC Cardiovasc Interv. 2015;8(7):927–36. doi:10.1016/j.jcin.2015.01.032.
27. Negi SI, Didier R, Ota H, Magalhaes MA, Popma CJ, Kollmer MR, et al. Role of near-infrared spectroscopy in intravascular coronary imaging. Cardiovasc Revasc Med. 2015;16(5):299–305. doi:10.1016/j.carrev.2015.06.001.
28. Madder RD, Steinberg DH, Anderson RD. Multimodality direct coronary imaging with combined near-infrared spectroscopy and intravascular ultrasound: initial US experience. Catheter Cardiovasc Interv. 2013;81(3):551–7. doi:10.1002/ccd.23358.
29. Madder RD, Wohns DH, Muller JE. Detection by intracoronary near-infrared spectroscopy of lipid core plaque at culprit sites in survivors of cardiac arrest. J Invas Cardiol. 2014;26(2):78–9.
30. Sinclair H, Bourantas C, Bagnall A, Mintz GS, Kunadian V. OCT for the identification of vulnerable plaque in acute coronary syndrome. JACC Cardiovasc Imaging. 2015;8(2):198–209. doi:10.1016/j.jcmg.2014.12.005.
31. Kubo T, Tanaka A, Ino Y, Kitabata H, Shiono Y, Akasaka T. Assessment of coronary atherosclerosis using optical coherence tomography. J Atheroscler Thromb. 2014;21(9):895–903.
32. Low AF, Tearney GJ, Bouma BE, Jang IK. Technology insight: optical coherence tomography–current status and future development. Nat Clin Pract Cardiovasc Med. 2006;3(3):154–62. doi:10.1038/ncpcardio0482 **(Quiz 72)**.
33. Jia H, Abtahian F, Aguirre AD, Lee S, Chia S, Lowe H, et al. In vivo diagnosis of plaque erosion and calcified nodule in patients with acute coronary syndrome by intravascular optical coherence tomography. J Am Coll Cardiol. 2013;62(19):1748–58. doi:10.1016/j.jacc.2013.05.071.
34. • Kini AS, Motoyama S, Vengrenyuk Y, Feig JE, Pena J, Baber U, et al. Multimodality intravascular imaging to predict periprocedural myocardial infarction during percutaneous coronary intervention. JACC Cardiovasc Interv. 2015;8(7):937–45. doi:10.1016/j.jcin.2015.03.016. *This article is important because it demonstrates that OCT-determined fibrous cap thickness is the best predictor for the occurrence of peri-procedural myocardial infarction during percutaneous coronary intervention. Thus, identification of this marker has the potential to prevent future complications.*
35. Prati F, Uemura S, Souteyrand G, Virmani R, Motreff P, Di Vito L, et al. OCT-based diagnosis and management of STEMI associated with intact fibrous cap. JACC Cardiovasc Imaging. 2013;6(3):283–7. doi:10.1016/j.jcmg.2012.12.007.
36. Nishio R, Shinke T, Otake H, Nakagawa M, Nagoshi R, Inoue T, et al. Stabilizing effect of combined eicosapentaenoic acid and statin therapy on coronary thin-cap fibroatheroma. Atherosclerosis. 2014;234(1):114–9. doi:10.1016/j.atherosclerosis.2014.02.025.
37. Roleder T, Jakala J, Kaluza GL, Partyka L, Proniewska K, Pociask E, et al. The basics of intravascular optical coherence tomography. Postepy Kardiol Interwencyjnej. 2015;11(2):74–83. doi:10.5114/pwki.2015.52278.
38. van Soest G, Regar E, Goderie TP, Gonzalo N, Koljenovic S, van Leenders GJ, et al. Pitfalls in plaque characterization by OCT: image artifacts in native coronary arteries. JACC Cardiovasc Imaging. 2011;4(7):810–3. doi:10.1016/j.jcmg.2011.01.022.
39. Magnoni M, Ammirati E, Camici PG. Non-invasive molecular imaging of vulnerable atherosclerotic plaques. J Cardiol. 2015;65(4):261–9. doi:10.1016/j.jjcc.2015.01.004.
40. Baumann S, Renker M, Meinel FG, Wichmann JL, Fuller SR, Bayer RR 2nd, et al. Computed tomography imaging of coronary artery plaque: characterization and prognosis. Radiol Clin North Am. 2015;53(2):307–15. doi:10.1016/j.rcl.2014.11.008.
41. •• Tesche C, Caruso D, De Cecco CN, Shuler DC, Rames JD, Albrecht MH, et al. Coronary computed tomography angiography-derived plaque quantification in patients with acute coronary syndrome. Am J Cardiol. 2017;119(5):712–8. doi:10.1016/j.amjcard.2016.11.030. *This article is of outstanding importance because it demonstrates that the presence of certain CT-derived atherosclerotic plaque features may allow for the stratification of patients at high risk of acute coronary disease. This has the potential to guide a more tailored therapy in clinical practice.*
42. Benedek T, Gyongyosi M, Benedek I. Multislice computed tomographic coronary angiography for quantitative assessment of culprit lesions in acute coronary syndromes. Can J Cardiol. 2013;29(3):364–71. doi:10.1016/j.cjca.2012.11.004.
43. Moscariello A, Vliegenthart R, Schoepf UJ, Nance JW Jr, Zwerner PL, Meyer M, et al. Coronary CT angiography versus conventional cardiac angiography for therapeutic decision making in patients with high likelihood of coronary artery disease. Radiology. 2012;265(2):385–92. doi:10.1148/radiol.12112426.
44. Nakazato R, Shalev A, Doh JH, Koo BK, Dey D, Berman DS, et al. Quantification and characterisation of coronary artery plaque volume and adverse plaque features by coronary computed tomographic angiography: a direct comparison to intravascular ultrasound. Eur Radiol. 2013;23(8):2109–17. doi:10.1007/s00330-013-2822-1.
45. Otsuka K, Fukuda S, Tanaka A, Nakanishi K, Taguchi H, Yoshikawa J, et al. Napkin-ring sign on coronary CT angiography for the prediction of acute coronary syndrome. JACC Cardiovasc Imaging. 2013;6(4):448–57. doi:10.1016/j.jcmg.2012.09.016.
46. Motwani M, Dey D, Berman DS, Germano G, Achenbach S, Al-Mallah MH, et al. Machine learning for prediction of all-cause mortality in patients with suspected coronary artery disease: a 5-year multicentre prospective registry analysis. Eur Heart J. 2017;38(7):500–7. doi:10.1093/eurheartj/ehw188.
47. Kristanto W, van Ooijen PM, Weide MC, Vliegenthart R, Oudkerk M. A meta-analysis and hierarchical classification of HU-based atherosclerotic plaque characterization criteria. PLoS ONE. 2013;8(9):e73460. doi:10.1371/journal.pone.0073460.
48. Patino M, Prochowski A, Agrawal MD, Simeone FJ, Gupta R, Hahn PF, et al. Material separation using dual-energy CT: current and emerging applications. Radiographics. 2016;36(4):1087–105. doi:10.1148/rg.2016150220.
49. Obaid DR, Calvert PA, Gopalan D, Parker RA, West NE, Goddard M, et al. Dual-energy computed tomography imaging to determine atherosclerotic plaque composition: a prospective study with tissue validation. J Cardiovasc Comput Tomogr. 2014;8(3):230–7. doi:10.1016/j.jcct.2014.04.007.

50. Henzler T, Porubsky S, Kayed H, Harder N, Krissak UR, Meyer M, et al. Attenuation-based characterization of coronary atherosclerotic plaque: comparison of dual source and dual energy CT with single-source CT and histopathology. Eur J Radiol. 2011;80(1):54–9. doi:10.1016/j.ejrad.2010.07.024.
51. Danad I, Fayad ZA, Willemink MJ, Min JK. New applications of cardiac computed tomography: dual-energy, spectral, and molecular CT imaging. JACC Cardiovasc Imaging. 2015;8(6):710–23. doi:10.1016/j.jcmg.2015.03.005.
52. Mannelli L, MacDonald L, Mancini M, Ferguson M, Shuman WP, Ragucci M, et al. Dual energy computed tomography quantification of carotid plaques calcification: comparison between monochromatic and polychromatic energies with pathology correlation. Eur Radiol. 2015;25(5):1238–46. doi:10.1007/s00330-014-3523-0.
53. Calcagno C, Ramachandran S, Millon A, Robson PM, Mani V, Fayad Z. Gadolinium-based contrast agents for vessel wall magnetic resonance imaging (MRI) of atherosclerosis. Curr Cardiovasc Imaging Rep. 2013;6(1):11–24. doi:10.1007/s12410-012-9177-x.
54. Huibers A, de Borst GJ, Wan S, Kennedy F, Giannopoulos A, Moll FL, et al. Non-invasive carotid artery imaging to identify the vulnerable plaque: current status and future goals. Eur J Vasc Endovasc Surg. 2015;50(5):563–72. doi:10.1016/j.ejvs.2015.06.113.
55. Brinjikji W, Huston J 3rd, Rabinstein AA, Kim GM, Lerman A, Lanzino G. Contemporary carotid imaging: from degree of stenosis to plaque vulnerability. J Neurosurg. 2016;2016(1):27–42. doi:10.3171/2015.1.JNS142452.test.
56. Yu W, Underhill HR, Ferguson MS, Hippe DS, Hatsukami TS, Yuan C, et al. The added value of longitudinal black-blood cardiovascular magnetic resonance angiography in the cross sectional identification of carotid atherosclerotic ulceration. J Cardiovasc Magn Reson. 2009;11:31. doi:10.1186/1532-429X-11-31.
57. den Hartog AG, Bovens SM, Koning W, Hendrikse J, Luijten PR, Moll FL, et al. Current status of clinical magnetic resonance imaging for plaque characterisation in patients with carotid artery stenosis. Eur J Vasc Endovasc Surg. 2013;45(1):7–21. doi:10.1016/j.ejvs.2012.10.022.
58. Fitzpatrick LA, Berkovitz N, Dos Santos MP, Majeed N, Glikstein R, Chakraborty S, et al. Vulnerable carotid plaque imaging and histopathology without a dedicated MRI receiver coil. Neuroradiol J. 2017;30(2):120–8. doi:10.1177/1971400916678244.
59. Puppini G, Furlan F, Cirota N, Veraldi G, Piubello Q, Montemezzi S, et al. Characterisation of carotid atherosclerotic plaque: comparison between magnetic resonance imaging and histology. Radiol Med. 2006;111(7):921–30. doi:10.1007/s11547-006-0091-7.
60. Gaens ME, Backes WH, Rozel S, Lipperts M, Sanders SN, Jaspers K, et al. Dynamic contrast-enhanced MR imaging of carotid atherosclerotic plaque: model selection, reproducibility, and validation. Radiology. 2013;266(1):271–9. doi:10.1148/radiol.12120499.
61. Millon A, Boussel L, Brevet M, Mathevet JL, Canet-Soulas E, Mory C, et al. Clinical and histological significance of gadolinium enhancement in carotid atherosclerotic plaque. Stroke. 2012;43(11):3023–8. doi:10.1161/STROKEAHA.112.662692.
62. Qiao Y, Etesami M, Astor BC, Zeiler SR, Trout HH 3rd, Wasserman BA. Carotid plaque neovascularization and hemorrhage detected by MR imaging are associated with recent cerebrovascular ischemic events. AJNR Am J Neuroradiol. 2012;33(4):755–60. doi:10.3174/ajnr.A2863.
63. van Hoof RH, Voo SA, Sluimer JC, Wijnen NJ, Hermeling E, Schreuder FH, et al. Vessel wall and adventitial DCE-MRI parameters demonstrate similar correlations with carotid plaque microvasculature on histology. J Magn Reson Imaging. 2017;. doi:10.1002/jmri.25648.
64. •• Gupta A, Baradaran H, Schweitzer AD, Kamel H, Pandya A, Delgado D, et al. Carotid plaque MRI and stroke risk: a systematic review and meta-analysis. Stroke. 2013;44(11):3071–7. doi:10.1161/STROKEAHA.113.002551. *This study is of outstanding importance because it demonstrates in a large patient population that MRIderived atherosclerotic carotid plaque features of vulnerability are associated with a significant increase in the risk of acute cerebrovascular events.*
65. Saam T, Hetterich H, Hoffmann V, Yuan C, Dichgans M, Poppert H, et al. Meta-analysis and systematic review of the predictive value of carotid plaque hemorrhage on cerebrovascular events by magnetic resonance imaging. J Am Coll Cardiol. 2013;62(12):1081–91. doi:10.1016/j.jacc.2013.06.015.
66. Sibley CT, Vavere AL, Gottlieb I, Cox C, Matheson M, Spooner A, et al. MRI-measured regression of carotid atherosclerosis induced by statins with and without niacin in a randomised controlled trial: the NIA plaque study. Heart. 2013;99(22):1675–80. doi:10.1136/heartjnl-2013-303926.
67. Yoshida K, Sadamasa N, Narumi O, Chin M, Yamagata S, Miyamoto S. Symptomatic low-grade carotid stenosis with intraplaque hemorrhage and expansive arterial remodeling is associated with a high relapse rate refractory to medical treatment. Neurosurgery. 2012;70(5):1143–50. doi:10.1227/NEU.0b013e31823fe50b **(Discussion 50–51)**.
68. •• Yoshimura S, Yamada K, Kawasaki M, Asano T, Kanematsu M, Miyai M, et al. Selection of carotid artery stenting or endarterectomy based on magnetic resonance plaque imaging reduced periprocedural adverse events. J Stroke Cerebrovasc Dis. 2013;22(7):1082–7. doi:10.1016/j.jstrokecerebrovasdis.2012.07.018. *This article is of outstanding importance because it demonstrates that, in patients with carotid atherosclerotic disease, MRI is a reliable tool in the decision-making process for future therapies and also allows the prediction of complications during and after revascularization procedures.*
69. Makowski MR, Henningsson M, Spuentrup E, Kim WY, Maintz D, Manning WJ, et al. Characterization of coronary atherosclerosis by magnetic resonance imaging. Circulation. 2013;128(11):1244–55. doi:10.1161/CIRCULATIONAHA.113.002681.
70. Evans NR, Tarkin JM, Chowdhury MM, Warburton EA, Rudd JH. PET imaging of atherosclerotic disease: advancing plaque assessment from anatomy to pathophysiology. Curr Atheroscler Rep. 2016;18(6):30. doi:10.1007/s11883-016-0584-3.
71. Hammad B, Evans NR, Rudd JH, Tawakol A. Molecular imaging of atherosclerosis with integrated PET imaging. J Nucl Cardiol. 2017;. doi:10.1007/s12350-016-0766-y.
72. Figueroa AL, Abdelbaky A, Truong QA, Corsini E, MacNabb MH, Lavender ZR, et al. Measurement of arterial activity on routine FDG PET/CT images improves prediction of risk of future CV events. JACC Cardiovasc Imaging. 2013;6(12):1250–9. doi:10.1016/j.jcmg.2013.08.006.
73. • Irkle A, Vesey AT, Lewis DY, Skepper JN, Bird JL, Dweck MR, et al. Identifying active vascular microcalcification by (18)F-sodium fluoride positron emission tomography. Nat Commun. 2015;6:7495. doi:10.1038/ncomms8495. *This article is important because it demonstrates that NaF-PET imaging allows for the discrimination between areas of macro and micro-calcification, the latter being associated with plaque rupture.*
74. Morbelli S, Fiz F, Piccardo A, Picori L, Massollo M, Pestarino E, et al. Divergent determinants of 18F–NaF uptake and visible calcium deposition in large arteries: relationship with Framingham risk score. Int J Cardiovasc Imaging. 2014;30(2):439–47. doi:10.1007/s10554-013-0342-3.
75. Fiz F, Morbelli S, Piccardo A, Bauckneht M, Ferrarazzo G, Pestarino E, et al. (1)(8)F-NaF uptake by atherosclerotic plaque on PET/CT imaging: inverse correlation between calcification

density and mineral metabolic activity. J Nucl Med. 2015;56(7):1019–23. doi:10.2967/jnumed.115.154229.
76. Derlin T, Richter U, Bannas P, Begemann P, Buchert R, Mester J, et al. Feasibility of 18F-sodium fluoride PET/CT for imaging of atherosclerotic plaque. J Nucl Med. 2010;51(6):862–5. doi:10.2967/jnumed.110.076471.
77. Dweck MR, Chow MW, Joshi NV, Williams MC, Jones C, Fletcher AM, et al. Coronary arterial 18F-sodium fluoride uptake: a novel marker of plaque biology. J Am Coll Cardiol. 2012;59(17):1539–48. doi:10.1016/j.jacc.2011.12.037.
78. Tawakol A, Fayad ZA, Mogg R, Alon A, Klimas MT, Dansky H, et al. Intensification of statin therapy results in a rapid reduction in atherosclerotic inflammation: results of a multicenter fluorodeoxyglucose-positron emission tomography/computed tomography feasibility study. J Am Coll Cardiol. 2013;62(10):909–17. doi:10.1016/j.jacc.2013.04.066.
79. Wu YW, Kao HL, Huang CL, Chen MF, Lin LY, Wang YC, et al. The effects of 3-month atorvastatin therapy on arterial inflammation, calcification, abdominal adipose tissue and circulating biomarkers. Eur J Nucl Med Mol Imaging. 2012;39(3):399–407. doi:10.1007/s00259-011-1994-7.
80. Calcagno C, Ramachandran S, Izquierdo-Garcia D, Mani V, Millon A, Rosenbaum D, et al. The complementary roles of dynamic contrast-enhanced MRI and 18F-fluorodeoxyglucose PET/CT for imaging of carotid atherosclerosis. Eur J Nucl Med Mol Imaging. 2013;40(12):1884–93. doi:10.1007/s00259-013-2518-4.
81. Saito H, Kuroda S, Hirata K, Magota K, Shiga T, Tamaki N, et al. Validity of dual MRI and F-FDG PET imaging in predicting vulnerable and inflamed carotid plaque. Cerebrovasc Dis. 2013;35(4):370–7. doi:10.1159/000348846.